Journal Pre-proofs

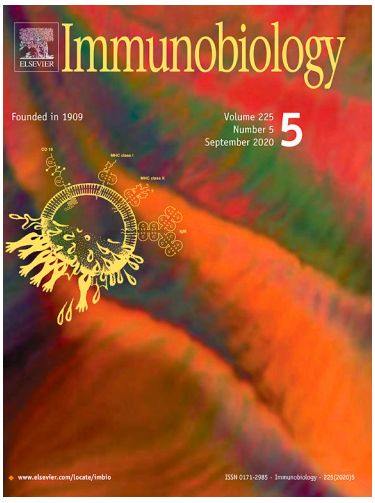

Chronic NOD2 stimulation by MDP confers protection against parthanatos through M2b macrophage polarization in RAW264.7 cells

Florencia C. Mansilla, María C. Miraglia, Silvina S. Maidana, Randazzo Cecilia, Alejandra V. Capozzo

PII: S0171-2985(24)00051-2
DOI: https://doi.org/10.1016/j.imbio.2024.152833
Reference: IMBIO 152833

To appear in: *Immunobiology*

Received Date: 26 February 2024
Revised Date: 24 June 2024
Accepted Date: 28 June 2024

Please cite this article as: F.C. Mansilla, M.C. Miraglia, S.S. Maidana, R. Cecilia, A.V. Capozzo, Chronic NOD2 stimulation by MDP confers protection against parthanatos through M2b macrophage polarization in RAW264.7 cells, *Immunobiology* (2024), doi: https://doi.org/10.1016/j.imbio.2024.152833

Chronic NOD2 stimulation by MDP confers protection against parthanatos through M2b macrophage polarization in RAW264.7 cells

Florencia C. Mansilla[1]*; María C. Miraglia[1,2]; Silvina S. Maidana[1,2]; Randazzo Cecilia[1]; Alejandra V. Capozzo[2,3]

[1] Institute of Virology and Technological Innovations, Center for Research in Veterinary and Agronomic Sciences (CICVyA), INTA, Buenos Aires, Argentina

[2] National Council for Scientific and Technical Research (CONICET)

[3] Center for Advanced Studies in Human Sciences and Health (CAECIHS), Interamerican Open University (UAI), Buenos Aires, Argentina

*Corresponding author: manslla.florencia@inta.gob.arInstitute of Virology and Technological Innovations, Center for Research in Veterinary and Agronomic Sciences (CICVyA), INTA-National Council for Technical Research (CONICET), N. Repetto y De Los Reseros s/n (1686), Hurlingham 1686, Buenos Aires, Argentina

The authors declare that they have no known competing financial interests or personal relationships that could have appeared to influence the work reported in this paper.

Abstract

Innate immune cells show enhanced responsiveness to secondary challenges after an initial non-related stimulation (Trained Innate Immunity, TII). Acute NOD2 activation by Muramyl-Dipeptide (MDP) promotes TII inducing the secretion of pro-inflammatory mediators, while a sustained MDP-stimulation down-regulates the inflammatory response, restoring tolerance. Here we characterized *in-vitro* the response of murine macrophages to lipopolysaccharide (LPS) challenge under NOD2-chronic stimulation. RAW264.7 cells were trained with MDP (1μg/ml, 48h) and challenged with LPS (5μg/ml, 24h). Trained cells formed multinucleated giant cells with increased phagocytosis rates compared to untrained/challenged cells. They showed a reduced mitochondrial activity and a switch to aerobic glycolysis. TNF-α, ROS and NO were upregulated in both trained and untrained cultures (MDP+, MDP- cells, $p>0.05$); while IL-10, IL-6 IL-12 and MHCII were upregulated only in trained cells after LPS challenge (MDP+LPS+, $p<0.05$). A slight upregulation in the expression of B7.2 was also observed in this group, although

differences were not statistically significant. MDP-training induced resistance to LPS challenge ($p<0.01$). The relative expression of PARP-1 was downregulated after the LPS challenge, which may contribute to the regulatory milieu and to the innate memory mechanisms exhibited by MDP-trained cells. Our results demonstrate that a sustained MDP-training polarizes murine macrophages towards a M2b profile, inhibiting parthanatos. These results may impact on the development of strategies to immunomodulate processes in which inflammation should be controlled.

Keywords: M2b macrophages, muramyl-dipeptide, NOD2, LPS resistance, PARP-1

1. Introduction

Emerging studies have demonstrated that innate immune cells have primitive immune memory mechanisms referred to as *Trained Innate Immunity* (Quintin et al., 2014), adapting non-specifically after a transient stimulation through metabolic and epigenetic modifications thus remaining with enhanced responsiveness to secondary challenges with a non-related stimuli (Netea et al., 2020, 2011). Even though trained innate immunity can be induced in all immune cell types and in some non-immune cell types, this concept was first stablished in monocyte-derived macrophages, inducing phenotypical polarization to mount specific functional programs (Hamada et al., 2019). During this process, macrophages adopt different functional characteristics in response to specific environmental contexts. This results in the differentiation of macrophages into two main types: classically activated (M1), induced by stimuli that can be structural units of different pathogens (such as LPS) or pro-inflammatory molecules secreted by other immune cells (IFN-γ), producing proinflammatory cytokines, nitric oxide, and reactive oxygen intermediates to combat pathogens; and alternatively activated (M2) macrophages, induced by cytokines such as IL-4, IL-10, or IL-13 and involved in wound healing, tissue repair, regulatory response and extracellular matrix formation. M2 macrophages are further differentiated into M2a, M2b, M2c, and M2d subtypes, each distinguished by unique cell surface markers, cytokines released and biological roles (Gordon, 2003; Van Ginderachter et al., 2006; Wang et al., 2019).

Muramyl dipeptide (MDP) is the minimal structural unit of bacterial peptidoglycan, which consists of N-acetylyglucosamine and N-acetylmuramic acid disaccharide chains linking the lactyl group of one N-acetylmuramic acid to the other, typically in L-alanine D-glutamine dipeptides (Ogawa et al., 2011). It is the major structural element of the cell walls of most bacteria that can elicit an immune response through the activation of NF-κB and MAPK signaling pathways resulting in the production of proinflammatory cytokines. In this context, the pro-inflammatory effect of muramyl dipeptide (MDP) is prototypical. MDP synergistically enhance the secretion of LPS-induced proinflammatory mediators after binding to NOD2 (Girardin et al., 2003), which is associated to the activation of neutrophils, monocytes, macrophages and lymphocytes (Guryanova and Khaitov, 2021). Interestingly, MDP can also regulate intracellular processes, triggering anti-inflammatory and regulatory responses to down-regulate inflammation, ensuring tolerance to microbiome and preventing septic shock (Guryanova, 2022). It was suggested that while acute NOD2 activation by MDP signals through NFκB and MAPK pathways, a sustained stimulation may promote NOD2 degradation, thus restoring both self- and cross-tolerizing effects (Guryanova and

Khaitov, 2021). The absence of tolerogenic responses may lead macrophages to parthanatos, an overproduction-related cell death program (Robinson et al., 2019) which relies on the hyper-activation of Poly [ADP-ribose] polymerase 1 (PARP-1) mediated by oxidative and nitrosative stress (Andrabi et al., 2008; David et al., 2009). Hence, the restoration of homeostasis after inflammation is paramount.

Peripheral monocytes and macrophages that enter mucosal sites are continuously exposed to both local and systemic effects of MDP present in the bloodstream because of the microbiome breakdown (Guryanova, 2022; Guryanova and Khaitov, 2021; Huang et al., 2019). However, the potential protective role of MDP-mediated chronic NOD2 stimulation considering its tolerogenic effect is not totally understood, as studies have mainly focused on functions after acute, rather than chronic NOD2 stimulation (Guryanova and Khaitov, 2021). Considering this, in this study we aimed to characterize *in vitro* the immune response of murine macrophages to an experimental LPS challenge in the context of chronic inflammation induced by a sustained stimulation of NOD2 using MDP.

2. Materials and Methods

2.1 Cells and treatments

RAW264.7 cells from the American Type Cell Collection (ATCC®) were cultured in Dulbecco's Modified Eagle's Medium (DMEM, Gibco®, Thermo Fisher, DE, USA) supplemented with fetal bovine serum (FBS) 10% (v/v), Hepes (10 mM), glutamine (2 mM) and 1% (v/v) of Gibco™ Antibiotic-antimycotic solution (100X, Gibco), containing penicillin 100 U/ml, streptomycin 100 µg/ml and Amphotericin B 0.25 µg/ml. Experiments were performed using the same batch of each reagent and cells were maintained no longer than fifteen passages to preserve culture identity (Taciak et al., 2018). Cells were gently detached with a scrapper and counted. A final volume 0.2 or 1 ml/well of supplemented DMEM containing 2 $x10^4$ or 2 $x10^5$ cells was seeded in 96 or 12 well plates, respectively. In each experiment, an aliquot containing $5x10^4$ cells was stained with a fluorescent probe as described below (section 2.4) to verify their viability (data not shown). After an ON resting period, cells were trained with 1 µg/ml of MDP (referred to as MDP+ cells, InvivoGen, CA, USA) and incubated for 48h at 37°C and 5% CO_2 in complete DMEM supplemented with 2% FBS. Then supernatants were removed and lipopolysaccharide from *Escherichia coli* O127:B8 (LPS, 5 µg/ml, Sigma Aldrich, MO, USA) in complete DMEM with 2% FBS was added (referred to as MDP+LPS+ cells). After 24h supernatants were collected and stored at -80°C until processing and cells were detached (if necessary) and processed. In each experiment, cells that were LPS challenged in the absence of training with MDP (MDP-LPS+) and a control group that was neither trained with MDP nor challenged (MDP-LPS-) were included.

2.2 Morphological and functional modifications induced by MDP

The induction of morphological modifications by MDP training was verified by Papanicolaou staining using a commercial kit (Tincion15, Biopur, Santa Fe, Argentina) following the manufacturer´s protocol. Briefly, sterile glass culture slides (Sigma Aldrich) were placed on 12 well plates, then 2 $x10^5$ cells in 1 ml of supplemented DMEM (10% FBS) were seeded in each well and incubated for 48h with MDP (1µg/ml) at 37°C with CO_2 5%. Then supernatants were discarded, glasses were washed with PBS 1x and carefully detached using a 25g needle. Each

glass was then sequentially immersed for 5 seconds in each one of the solutions provided by the manufacturer (fixative solution, solution 1 containing xanthinic dyes and solution 2 containing thiazine dyes). Glasses were then washed with running water and air dried, before being observed under optical microscope. Giant multinucleated cells were quantified in five randomly obtained pictures of each treatment using ImageJ (Hartig, 2013).

The phagocytic ability of the trained cells in response to LPS challenge (MDP+LPS+) was measured by neutral red uptake following manufacturer´s instructions. Supernatants were removed and preserved at -80°C and 100 µl of neutral red solution (0.075% w/v) in PBS 1x, Sigma Aldrich) was added to each well using 96-well plates. Plates were incubated for 2h at 37°C, washed twice with PBS 1x (250 µl/well) and incubated with 150 µl/well of a destaining solution (ethanol: H_2O: acetic acid, 50:49:1) at 37°C for 10 min with constant agitation. OD_{540} was determined by spectrophotometry.

The XTT reducing activity was assessed using a commercial kit (TACS® XTT Cell Proliferation Assay Kit, BioTechne, CA, USA) according to manufacturer´s instructions. Briefly, 50 µl/well of working solution (xtt activator: xtt reagent, 1:50) were added to each well from 96-well plates. Cells were incubated for 2h at 37°C and 5% CO_2 and OD_{490} was determined by spectrophotometry.

The glucose intake was assessed enzymatically using a commercial reagent containing glucose oxidase, peroxidase and 4-aminophenazone (Glucose, Biosystems S.A.S., Colombia). Supernatants previously collected (10 µl) were incubated with 1ml of the commercial reagent at 37°C for 5 min. OD_{505} was determined using a spectrophotometer.

2.3 Cytokine production and expression of MHCII and B7.2

The production of TNF-α, IL-10, IL-12 and IL-6 was determined by ELISA using commercial kits (BD OptEIA™ ELISA sets, BD, NJ, USA). Briefly, ELISA plates were incubated with capture antibody ON at 4°C. Then plates were washed with PBS-Tween 0.05% (3x, 250 µl/well), blocked (PSB-FBS 10%, 200 µl/well, 1h at room temperature) and undiluted supernatants were seeded (100 µl/well) and incubated for 2h at room temperature. After this incubation step, plates were washed with PBS-Tween 0.05% (5x, 250 µl/well) and both the detector antibody and the secondary antibody conjugated to peroxidase were added together, following manufacturer´s instructions (diluted 1:250, 100 µl/well, 1h at room temperature). Plates were washed again (7x, 250 µl/well) and a substrate solution containing TMB was added (100 µl/well, BD). After an incubation of 30 min at room temperature in dark, stop solution (H_2SO_4 2 N, 50 µl/well) was added and OD_{450} was determined. Results were compared to a standard curve.

Expression of MCHII and B7.2 on cell membrane were detected using FITC-conjugated anti-Mouse I-A[d] and anti-Mouse CD86 antibodies (BD). Briefly, $1x10^6$ cells were resuspended in 20 µl of staining buffer (PBS-FBS 2%) and 0.5 µg of each antibody was added on separated tubes. Cells were incubated for 15 min at 4°C, washed twice with PBS 1x (5 min at 800g), and fixed with 100 µl of paraformaldehyde (PFA) 0.2% (w/v). Cells were analyzed by flow cytometry using a FACSCalibur™ flow cytometer (Becton Dickinson Immunocytometry Systems™, San Diego, USA). Isotype-matched control antibodies were used, and a gate was defined in the analysis to exclude non-viable cells and debris. SSC vs FL1 data were acquired. Results were analyzed using FlowJo_V10 software (BD) and dot plots were obtained showing the percentage of positive events.

2.4 Determination of Reactive Species and membrane integrity

The production of Nitric Oxide (NO) was quantified spectrophotometrically using Griess Reagent Kit (Biotium, CA, USA) in the supernatant of trained or untrained challenged cells (MDP+LPS+ or MDP-LPS+, respectively). Samples (150 µl) were incubated with 20 µl of the commercial reagent and 130 µl of distilled water for 30 min at room temperature and OD_{548} was determined using a spectrophotometer. Results were compared to a standard curve.

Total Reactive Oxygen Species (ROS) were measured using a commercial kit based on intracellular staining with DCFDA/H2DCFDA (Total Reactive Oxygen Species (ROS) Assay Kit 520 nm, Thermo Fisher). Briefly, $1x10^6$ cells were resuspended in 100 µl of a solution containing DCFDA/H2DCFDA diluted 1:500 in PBS 1x. Cells were incubated at 37°C for 1h, washed (2x) in PBS 1x and fixed with PFA 0.2% (w/v).

Viability was determined by assessing membrane integrity with a commercial probe (LIVE/DEAD Viability/Cytotoxicity Kit, Thermo Fisher), which was diluted 1:1000 in PBS 1x. $1x10^6$ cells were resuspended in 500 µl of this solution and incubated for 15 min at 4°C. Cells were then washed (2x in 1ml of PBS), fixed with 100 µl of PFA 0.2% (w/v) and analyzed by flow cytometry. Cells were identified by their forward scatter properties and FSC vs FL4 were analyzed and the subpopulation of cells with lower intensity were gated ("LIVE"). Results were analyzed using FlowJo_V10 software (BD) and dot plot for FSC vs FL4 were obtained, indicating the percentage of live cells (%).

2.5 Relative expression levels of PARP-1

RNA from trained or untrained challenged cells (MDP+LPS+ or MDP-LPS+) was extracted following a standard protocol using Biozol reagent (Pb-L, Buenos Aires, Argentina). Unchallenged cells, with or without pervious MDP training (MDP+LPS- and MDP-LPS-, respectively) were included as controls. RNA samples were digested with DNAse (1 µg/each with 1U of RQ1, Promega, WI, USA) for 30 min at 37°C. Then RQ1 stop solution was added and incubated for 10 min at 65°C for enzyme inactivation. The integrity of extracted RNA samples was verified by electrophoresis. Samples were incubated with M-MLV (200 U/sample, Promega) for 1h at 42°C for reverse transcription followed by 10 min at 94°C for enzyme inactivation (Promega). RNA purity and quantity was determined using a spectrophotometer ($260_{nm}/280_{nm}$).

The relative expression of PARP-1 was assessed by Real Time PCR using previously described primers (Fw: GGAGCTGCTCATCTTCAACC; Rv: GCAGTGACATCCCCAGTACA; Regdon et al., 2019). B-actin was used as reference gen (Fw: 5'-GAGACCTTCAACACCCCAGC-3'; Rv: 5'-ATGTCACGCACGATTTCCC-3'). Amplifications were performed using Mix qPCR SYBR/ROX (Pb-L) and following a standard reaction (95°C for 10 min and 40 cycles at 95°C for 30s, 60°C for 30s, 72°C for 30s for termination). Melting curve analysis was conducted after each cycle (StepOne, Applied Biosystems, Thermo Fisher). The delta-delta CT method was used to determine the relative expression of PARP-1, as previously described (Livak and Schmittgen, 2001). Briefly, the average Ct value for PARP-1 and β-Actin and the ΔCt values in each experimental (MDP+LPS+; MDP+LPS- or MDP-LPS+) and control condition (MDP-LPS-) was calculated. Then, the difference in gene expression between experimental and control samples was obtained (ΔΔCt) subtracting the ΔCt value of the control sample from the ΔCt value of the experimental samples. This value was then used to calculate the fold change in gene expression between the samples ($2^{-\Delta\Delta Ct}$).

2.6 Statistical analysis

All determinations were carried out in three independent experiments with three replicates each. Comparisons between groups were assessed by One Way ANOVA followed by Tukey Test to evaluate significant differences between groups (95% CI). Graphpad Prism 9.0 software was used.

3 Results

3.1 Metabolic and morphologic effects of chronic NOD2 stimulation

The optimal concentration of LPS was experimentally determined. Increased phagocytosis activity was observed in cells challenged either with 5 or 10 μg/ml of LPS, while no differences were found in cells challenged with 1 μg/ml of LPS compared to unchallenged cells (Fig. 1a, $p<0.05$). The XTT reduction activity was not affected by LPS challenge within the range evaluated (1-10 μg/ml; Fig. 1b, $p>0.05$), compared with unchallenged cells.

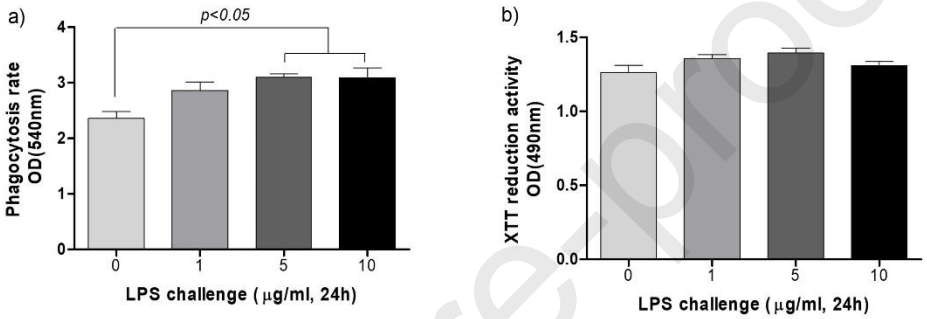

Fig. 1. Set up of experimental LPS challenge. RAW264.7 cells were experimentally challenged with increasing amounts of LPS (0-10 μg/ml) and incubated for 24h at 37°C and 5% CO_2. The phagocytic (a) and XTT reduction activity (b) of LPS challenged cells was assessed spectrophotometrically. Results from three independent experiments with three replicates each are depicted. Comparisons between groups were determined by One-Way ANOVA followed by Tukey post-test. Significant differences are depicted ($p<0.05$)

The presence of multinucleated giant cells, indicative of chronic inflammation, was verified by Papanicolaou staining (Fig. 2a and 2b) in MDP-trained cells (MDP+, 48h). After counting giant cells from 5 randomly taken photographs, an average value of 20 cells was observed in response to MDP training. This increase was statistically significant compared to untrained cells (MDP-), in which an average of 2.8 giant cells were counted ($p<0.001$).

RAW264.7 cells (MDP+ or MDP-) were then experimentally challenged with high doses of LPS (5 ug/ml) for 24h, as previously standardized.

The phagocytic activity of MDP+LPS+ cells was determined assessing neutral red intake levels. No differences were observed between MDP+LPS+ and MDP-LPS+ cells. However, our results showed an upregulation of phagocytosis induced by LPS challenge in both trained and untrained cells (MDP+LPS+ and MDP-LPS+, respectively; Fig. 2c) with statistically significant differences compared to MDP-LPS- cells ($p<0.05$). A reduced mitochondrial activity, inferred by a decreased XTT reduction activity ($p<0.05$), and higher consumption rates of glucose were also observed after LPS experimental challenge but only in MDP-trained cells (MDP+LPS+, Fig. 2d and 2e, respectively).

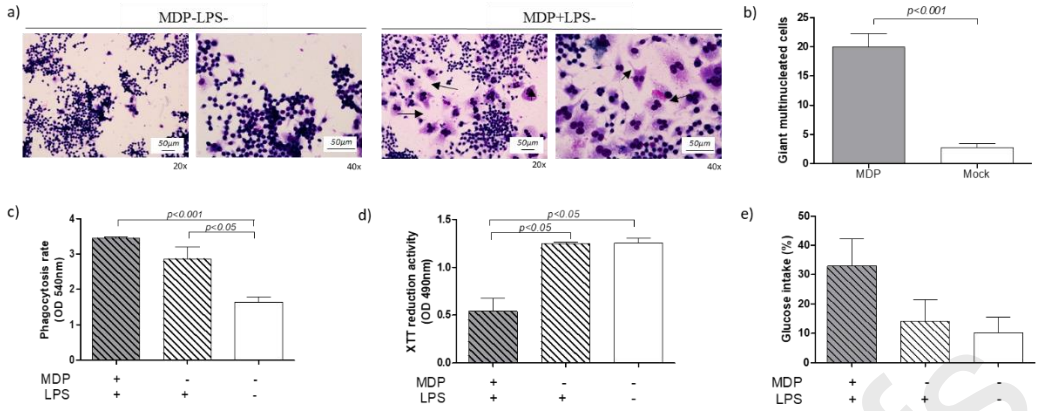

Fig. 2. Metabolic and morphologic effects of chronic NOD2 stimulation. The effect of a sustained MDP training on RAW264.7 cells was determined. a) Representative images of untrained (MDP-LPS-, left panel) vs MDP-trained (MDP+LPS-, right panel) cells are shown under 20x and 40x objective lens. Papanicolaou-stained giant multinucleated cells are depicted (black arrows). b) Giant multinucleated cells were quantified (ImageJ, NIH). Five pictures were randomly obtained from MDP-trained (MDP+LPS-) or untrained cells (MDP-LPS-) and the number of giant multinucleated cells under each condition was determined. Phagocytosis rates inferred from neutral red intake and XTT reduction activity (c and d, respectively) of MDP trained or untrained cells were determined after LPS experimental challenge (MDP+LPS+ and MDP-LPS-, respectively). Untrained/unchallenged cells (MDP-LPS-) were left as control cells. e) The glucose consumption under each experimental condition was also determined in an enzymatic assay. Results from three independent experiments with three replicates each are shown. Differences between groups were determined by One Way ANOVA followed by Tukey Test. Mean values ± SD and significance levels are depicted.

3.2 Cytokines production and expression of activation markers

The expression of different cytokines in the supernatant of trained cells that were experimentally challenged with LPS (MDP+LPS+) was determined by ELISA. TNF-α levels were upregulated by LPS without significant differences between MDP-trained (MDP+LPS+) or untrained cells (MDP-LPS+, Fig. 3a). Increased levels of IL-10, IL-6 and IL-12 were also detected after LPS challenge only in MPD-trained cells (MDP+LPS+, Fig. 3b, 3c and 3d, respectively; $p<0.05$).

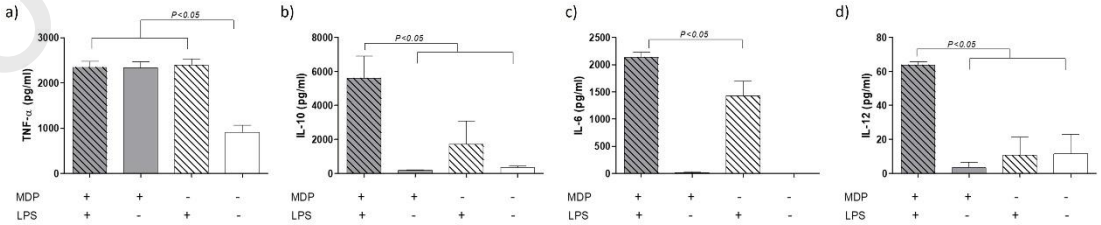

Fig 3. Cytokine production. The production of TNF-α (a), IL-10 (b), IL-12 (c) and IL-6 (d) was quantified in the supernatant of trained and untrained RAW264.7 cells after LPS challenge (MDP+LPS+ and MDP-LPS+, respectively) by ELISA using a commercial kit. Untrained/unchallenged cells (MDP-LPS-) were left as control. Statistical differences between treatments determined by One Way ANOVA followed by Tukey Test and the level of significance are depicted.

Results from three independent experiments with three replicates each are shown. Mean values ± SD are plotted.

The expression of MHCII and B7.2 on trained cells and its modulation in response to LPS challenge by flow cytometry was assessed. Our results showed a strong upregulation of MHCII induced by MDP sustained training after LPS challenge (MDP+LPS+ cells), with significant differences compared to the other experimental groups (MDP-LPS+; MDP+LPS- and MDP-LPS- cells; Fig 4a and 4b; $p<0.05$). Increased levels of B7.2 was also observed in MDP+LPS+ cells, although differences were not statistically significant (Fig. 4c and 4d; $p<0.05$).

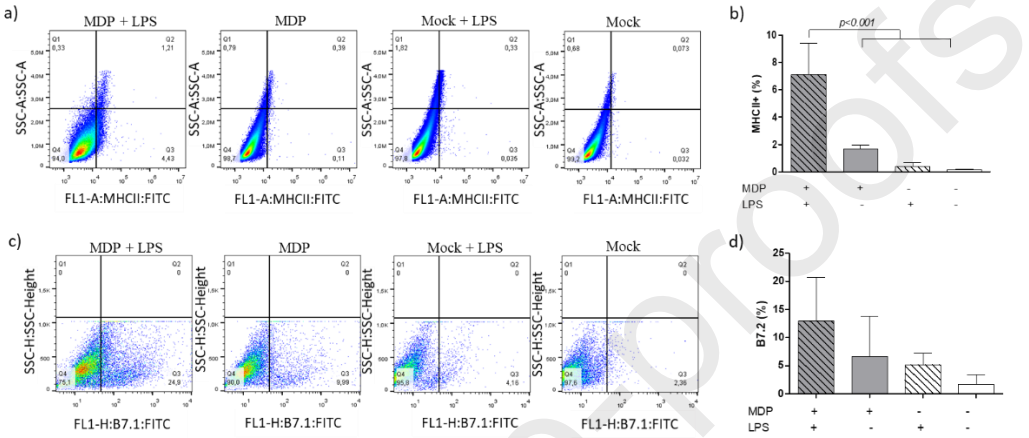

Fig 4. Upregulation of MHCII and B7.2. Trained and untrained RAW264.7 cells were stained with specific surface markers to determine the expression of MHCII and B7.2 after LPS experimental challenge (MDP+LPS+ or MDP-LPS+) by flow cytometry. Schematic representation of the modulation of the expression of MHCII and B7.2 under different experimental conditions (a and c, respectively). The percentage of cells expressing MHCII (b) and B7.2 (c) on their surface (%) is depicted. Trained and untrained/unchallenged cells (MDP+LPS- and MDP-LPS-, respectively) were left as control. Statistical differences determined by One-Way ANOVA followed by Tukey Test and the level of significance between groups are shown. Results from three independent experiments with three replicates each are depicted. Mean values ± SD are plotted.

The production of ROS and NO was quantified in trained cells after LPS challenge using a fluorescent stain or Griess Reaction, respectively. LPS challenge induced high levels of both ROS and NO, without differences between trained (MDP+LPS+) and untrained cells (MDP-LPS+, Fig. 5a and b).

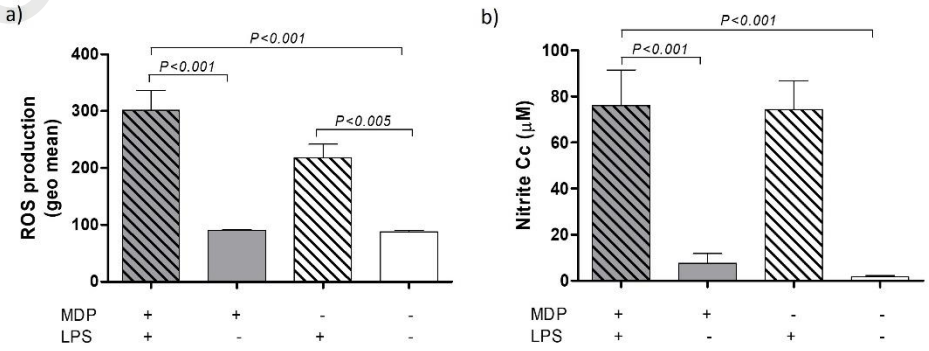

Fig 5. Production of oxygen and nitrogen reactive species. The production of ROS (a) and nitric oxide (b) was determined using DCFDA/H2DCFDA staining

and Griess Reaction, respectively, in trained and un-trained cells after LPS challenge (MDP+LPS+ or MDP-LPS+). Unchallenged cells (both MDP+LPS- and MDP-LPS-) were left as controls. Statistic differences assessed by One-Way ANOVA followed by Tukey Test and the level of significance between groups are shown. Results from three independent experiments with three replicates each are shown. Mean values ± SD are plotted.

3.3 Resistance to LPS challenge

The viability of MDP-trained cells after LPS challenge (MDP+LPS+) was inferred assessing membrane integrity using a fluorescent probe. The percentage of live cells was determined under each experimental condition by flow cytometry. An increase in the number of live cells was observed in MDP-trained cells in response to LPS (MDP+LPS+), compared to untrained challenged cells (MDP-LPS+); indicating a protective effect induced by MDP training associated with greater resistance to the experimental challenge. (Fig. 6a and 6b, $p<0.001$).

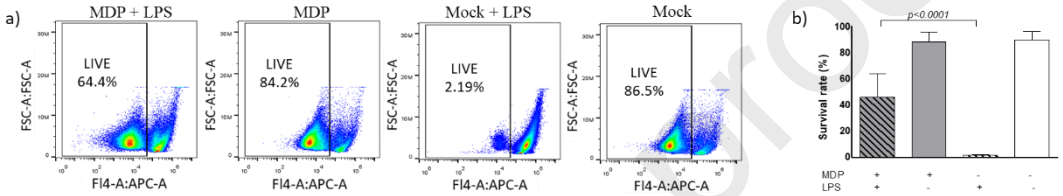

Fig 6. Resistance to LPS challenge. MDP trained and untrained RAW264.7 cells were experimentally challenged with LPS (MDP+LPS+ and MDP-LPS+, respectively). Trained/unchallenged (MDP+LPS-) and untrained/unchallenged cells (MDP-LPS-) were left as controls. a) Schematic representation of the survival rate under each experimental condition, according to membrane integrity assessment by flow cytometry. b) Survival rate of cells under different experimental treatments after LPS challenge. Results were obtained from three independent experiments with three replicates each. Mean values ± SD are plotted.

3.4 Relative expression of PARP-1

To explore possible mechanisms involved in the LPS resistance observed, the relative expression of PARP-1, an early responder in the DNA damage response whose inhibition induces trained innate immunity and protects from endotoxemia, was determined by real time PCR. The integrity of the extracted RNAs and absence of genomic DNA after DNase digestion was verified by electrophoresis in an agarose gel (data not shown). Our results suggest that PARP-1 is significantly downregulated after LPS experimental challenge in both MDP+LPS+ and MDP-LPS+ ($p<0.05$) and that this downregulation is significantly deepened when challenged cells were previously trained with MDP (MDP+LPS+ cells, Fig. 7, $p<0.001$). An increase in the expression levels of PARP-1 induced by MDP treatment prior to the LPS challenge (MDP+LPS-) was also observed. This suggests a central role of PARP-1 in the MDP-mediated resistance to LPS challenge.

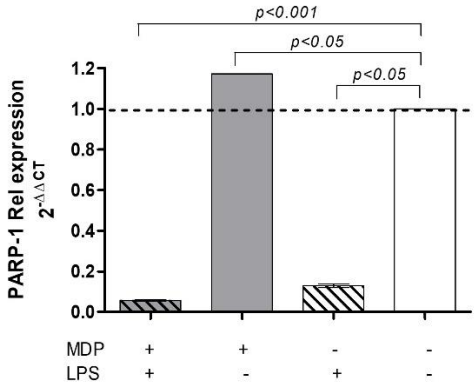

Fig 7. Relative PARP-1 expression. The relative PARP-1 expression was assessed by real time PCR in both trained and untrained RAW264.7 cells after LPS challenge (MDP+LPS+ and MDP-LPS+, respectively) according to the $2^{-\Delta\Delta Ct}$ method. Untrained/challenged (MDP-LPS+) and untrained/unchallenged (MDP-LPS-) cells were left as controls. Comparisons between groups were determined by One Way ANOVA followed by Tukey Post-test. Average values from three independent experiments with three replicates each are shown. Mean values ± SD are plotted.

4 Discussion

Trained Innate Immune response plays a key emerging role in the control of several diseases. However, it is now known that wrong or excessive trained innate immunity induction can cause an undesired effect, leading to unfavorable outcomes (Mishra et al., 2022; Netea et al., 2020). A single compound can exhibit great variation on its stimulating capacity depending on the source from which it is obtained, mass and schedule of administration (Byrne et al., 2021). Thus, trained innate immunity response and the concomitant macrophage polarization constitute a versatile target to control a broad spectrum of immunologic scenarios, including not only infectious, metabolic and inflammatory diseases, but also those in which anti-inflammatory or tolerogenic responses are needed to guarantee the restoration of homeostasis (Arts et al., 2018; Cárdenas-Tueme et al., 2020; Leentjens et al., 2018). Considering the pivotal role of MDPs in the modulation of different aspects of the immune response, we developed a model in which the effect of chronic NOD2 stimulation and its response against LPS challenge could be characterized *in vitro* using RAW264.7 cells. Although the use of cell lines has certain limitations, it is generally accepted that these cells are comparable to primary cultures of macrophages in terms of their ability to reproduce phagocytosis and immunomodulatory effects of different medications or immunomodulators (Baek et al., 2020; Elisia et al., 2018; Wei et al., 2022).

Our results demonstrate a strong macrophage polarization towards an M2b profile. These macrophages are involved in the resolution of inflammation through anti-inflammatory and/or regulatory functions, which can result in either protective or pathogenic outcomes in different disorders. They were first characterized in 2002 and, since then, different markers have been proposed (Anderson and Mosser, 2002; Martinez et al., 2008). Recently, Wang et al defined this phenotype as IL-10+, IL-12−, IL-6+, TNF-α+, CD11b+, MHCII+ cells (Wang et al., 2019). Our results evidenced an upregulation of both TNF-α and IL-10, reported as the main markers for M2b phenotype (Wang et al.,

2019). It was described that later phases of macrophage responses to TNF-α upregulate IL-10 production which induces cross-tolerance to subsequent TLR stimulation, thereby suppressing excessive pro-inflammatory cytokine production (Huynh et al., 2016; Park et al., 2011). M2b macrophages also inhibit conversion from quiescent M0 to M1, promoting tolerance (Wang et al., 2019). Thus, the induction of this profile by a chronic stimulation of NOD2 mediated by MDP, which is present in most bacteria, may have evolve as a protective strategy to avoid the induction of antimicrobial response.

The observed upregulation of both MHCII as well as the detection of high levels of IL-6 and low levels of IL-12, which is negatively regulated by IL-10 (Ma et al., 2015), were also indicative of an M2b profile. The expression of B7.2 was also upregulated by MDP, but differences were not statistically significant (Mantovani et al., 2004; Martinez et al., 2008; Yu et al., 2016).

The increased phagocytosis rates and decreased mitochondrial activity observed in MDP+LPS+ cells suggest a metabolic switch to aerobic glycolysis which was further supported by increased levels of glucose intake in those cells. This is usually induced by the free radicals produced under hypoxic conditions and contributes to macrophage activation (Kelly and O'Neill, 2015; Liu et al., 2012; Rodríguez-Prados et al., 2010; Wang et al., 2021). The presence of multinucleated giant cells, hallmark of chronic inflammation, was also evidenced after MDP training, although less is known about both their biological and functional activities in the context of macrophage polarization (Ahmadzadeh et al., 2022).

The LPS-induced production of both NO and ROS in RAW264.7 cells was previously reported, although different LPS concentrations were used in those studies (Aldridge et al., 2008; Asgharpour et al., 2019; Baek et al., 2020). In our model, no differences in NO or ROS levels between trained and untrained challenged cells (MDP+LPS+ and MDP-LPS+, respectively) were detected. Reactive species mediate different cellular processes and are one of the main actors of macrophages´ microbicide activity (Aldridge et al., 2008). However, it is known that an excessive or prolonged production of RNS/ROS is associated to tissue damage (Guzik et al., 2003; MacMicking et al., 1997), which is detrimental or even lethal to the cells, unless regulatory mechanisms are triggered (Regdon et al., 2019).

Considering these results, we aimed to determine the survival rate of cells exposed under high levels of nitrosative and oxidative stress. Despite most of the untrained cells (MDP-LPS+) faced death after challenge, a remarkable level of LPS resistance was observed induced by MDP training (MDP+LPS+). Parthanatos was previously verified in RAW264.7 cells and it was also demonstrated that PARP-1 inhibitors significantly reduced LPS-mediated cell death in mice both *in vivo* and in RAW264.7 cells, verifying the cross-talk between parthanatos and PARP-1 in endotoxemia (Xue et al., 2021). It was also reported that in M1 macrophages, sustained oxidative stress can lead to parthanatos, which is interestingly mitigated by LPS, suppressing PARP-1, boosting antioxidant proteins, and switching from mitochondrial respiration to aerobic glycolysis for energy production (Regdon et al., 2019). However, macrophages´ plasticity and particularly the role of M2b macrophages in parthanatos, remain unexplored. MDP treatment induced an upregulation of PARP-1 relative expression in unchallenged cells (MDP+LPS-). However, in response to LPS challenge both MDP+ and MDP- cells expressed significantly lower levels of PARP-1 than unchallenged cells (MDP+LPS- and MDP-LPS-). MDP training intensified this downregulation (in MDP+LPS cells), with

significant differences compared to MDP-LPS-. This may contribute to the regulatory milieu and to the innate memory mechanisms exhibited by MDP-trained cells.

PARP-1 has a complex and apparently promiscuous role in both pro-inflammatory processes downstream NfκB and DNA damage responses repairing DNA lesions induced by oxidative stress. The impact of PARP-1 suppression on cellular response to cytotoxic stimuli may depend on the severity of cellular stress. Given its dual function in regulating cell death, it is believed that under moderate DNA damage, its inhibition may enhance cellular susceptibility to parthanatos by disrupting DNA repair mechanisms. On the other hand, under extreme stress conditions with irreparable DNA breakage, PARP-1 downregulation seems to protect cells from necrosis (Regdon et al., 2019). Furthermore, PARP-1 inhibition induces trained innate mechanisms (Kim et al., 2020; Swindall et al., 2013), as oxidized DNA fragments translocate from the nucleus to the cytosol activating TLR9 signaling pathway (Liu et al., 2015). Hence, MDP-induced PARP-1 downregulation after LPS challenge and the subsequent impairment of the DNA Damage response may contribute to trained innate immune mechanisms triggered by NOD2, probably in collaboration with TLR9. Even though the synergistic activation of NODs and TLRs was already suggested by different authors (Pashenkov et al., 2019; Underhill, 2007), this should be further studied in this context.

Our results showed that chronic NOD2 stimulation mediated by MDP induces a regulatory effect, promoting an M2b phenotype which confers protection against parthanatos in RAW264.7 cells after a secondary LPS-challenge. Therefore, unraveling trained innate immunity mechanisms and macrophage polarization triggered by pattern recognition receptor (PRR) stimulation in different contexts emerges a powerful tool to develop high-potential strategies aimed at modulating immunological disorders.

5 Bibliography

Ahmadzadeh, K., Vanoppen, M., Rose, C.D., Matthys, P., Wouters, C.H., 2022. Multinucleated Giant Cells: Current Insights in Phenotype, Biological Activities, and Mechanism of Formation. Front. cell Dev. Biol. 10. https://doi.org/10.3389/FCELL.2022.873226

Aldridge, C., Razzak, A., Babcock, T.A., Helton, W.S., Espat, N.J., 2008. Lipopolysaccharide-stimulated RAW 264.7 macrophage inducible nitric oxide synthase and nitric oxide production is decreased by an omega-3 fatty acid lipid emulsion. J. Surg. Res. 149, 296–302. https://doi.org/10.1016/J.JSS.2007.12.758

Anderson, C.F., Mosser, D.M., 2002. A novel phenotype for an activated macrophage: the type 2 activated macrophage. J. Leukoc. Biol. 72, 101–106. https://doi.org/10.1189/JLB.72.1.101

Andrabi, S.A., Dawson, T.M., Dawson, V.L., 2008. Mitochondrial and nuclear cross talk in cell death: parthanatos. Ann. N. Y. Acad. Sci. 1147, 233–241. https://doi.org/10.1196/ANNALS.1427.014

Arts, R.J.W., Joosten, L.A.B., Netea, M.G., 2018. The potential role of trained immunity in autoimmune and autoinflammatory disorders. Front. Immunol. 9, 339966.

https://doi.org/10.3389/FIMMU.2018.00298/BIBTEX

Asgharpour, F., Moghadamnia, A.A., Motallebnejad, M., Nouri, H.R., 2019. Propolis attenuates lipopolysaccharide-induced inflammatory responses through intracellular ROS and NO levels along with downregulation of IL-1β and IL-6 expressions in murine RAW 264.7 macrophages. J. Food Biochem. 43. https://doi.org/10.1111/JFBC.12926

Baek, S.H., Park, T., Kang, M.G., Park, D., 2020. Anti-Inflammatory Activity and ROS Regulation Effect of Sinapaldehyde in LPS-Stimulated RAW 264.7 Macrophages. Molecules 25. https://doi.org/10.3390/MOLECULES25184089

Byrne, K.A., Tuggle, C.K., Loving, C.L., 2021. Differential induction of innate memory in porcine monocytes by β-glucan or bacillus Calmette-Guerin. Innate Immun. 27, 448–460. https://doi.org/10.1177/1753425920951607

Cárdenas-Tueme, M., Montalvo-Martínez, L., Maldonado-Ruiz, R., Camacho-Morales, A., Reséndez-Pérez, D., 2020. Neurodegenerative Susceptibility During Maternal Nutritional Programing: Are Central and Peripheral Innate Immune Training Relevant? Front. Neurosci. 14, 513057. https://doi.org/10.3389/FNINS.2020.00013/BIBTEX

David, K.K., Andrabi, S.A., Dawson, T.M., Dawson, V.L., 2009. Parthanatos, a messenger of death. Front. Biosci. (Landmark Ed. 14, 1116–1128. https://doi.org/10.2741/3297

Elisia, I., Pae, H.B., Lam, V., Cederberg, R., Hofs, E., Krystal, G., 2018. Comparison of RAW264.7, human whole blood and PBMC assays to screen for immunomodulators. J. Immunol. Methods 452, 26–31. https://doi.org/10.1016/J.JIM.2017.10.004

Girardin, S.E., Boneca, I.G., Viala, J., Chamaillard, M., Labigne, A., Thomas, G., Philpott, D.J., Sansonetti, P.J., 2003. Nod2 Is a General Sensor of Peptidoglycan through Muramyl Dipeptide (MDP) Detection *. J. Biol. Chem. 278, 8869–8872. https://doi.org/10.1074/JBC.C200651200

Gordon, S., 2003. Alternative activation of macrophages. Nat. Rev. Immunol. 2003 31 3, 23–35. https://doi.org/10.1038/nri978

Guryanova, S. V., 2022. Regulation of Immune Homeostasis via Muramyl Peptides-Low Molecular Weight Bioregulators of Bacterial Origin. Microorganisms 10. https://doi.org/10.3390/MICROORGANISMS10081526

Guryanova, S. V., Khaitov, R.M., 2021. Strategies for Using Muramyl Peptides - Modulators of Innate Immunity of Bacterial Origin - in Medicine. Front. Immunol. 12, 1339. https://doi.org/10.3389/FIMMU.2021.607178/BIBTEX

Guzik, T., Korbut, R., Adamek-Guzik, T., 2003. Nitric oxide and superoxide in inflammation and immune regulation. J. Physiol. Pharmacol.

Hamada, A., Torre, C., Drancourt, M., Ghigo, E., 2019. Trained immunity carried by non-immune cells. Front. Microbiol. 10, 3225.

https://doi.org/10.3389/FMICB.2018.03225/BIBTEX

Hartig, S. 2013. Basic image analysis and manipulation in ImageJ. Curr Protoc Mol Biol. 14,14-15. https://doi.org/10.1002/0471142727.mb1415s102.

Huang, Z., Wang, J., Xu, X., Wang, H., Qiao, Y., Chu, W.C., Xu, S., Chai, L., Cottier, F., Pavelka, N., Oosting, M., Joosten, L.A.B., Netea, M., Ng, C.Y.L., Leong, K.P., Kundu, P., Lam, K.P., Pettersson, S., Wang, Y., 2019. Antibody neutralization of microbiota-derived circulating peptidoglycan dampens inflammation and ameliorates autoimmunity. Nat. Microbiol. 4, 766–773. https://doi.org/10.1038/S41564-019-0381-1

Huynh, L., Kusnadi, A., Park, S.H., Murata, K., Park-Min, K.H., Ivashkiv, L.B., 2016. Opposing regulation of the late phase TNF response by mTORC1-IL-10 signaling and hypoxia in human macrophages. Sci. Rep. 6. https://doi.org/10.1038/SREP31959

Kelly, B., O'Neill, L.A.J., 2015. Metabolic reprogramming in macrophages and dendritic cells in innate immunity. Cell Res. 2015 257 25, 771–784. https://doi.org/10.1038/cr.2015.68

Kim, C., Wang, X.D., Yu, Y., 2020. PARP1 inhibitors trigger innate immunity via PARP1 trapping-induced DNA damage response. Elife 9, 1–47. https://doi.org/10.7554/ELIFE.60637

Leentjens, J., Bekkering, S., Joosten, L.A.B., Netea, M.G., Burgner, D.P., Riksen, N.P., 2018. Trained Innate Immunity as a Novel Mechanism Linking Infection and the Development of Atherosclerosis. Circ. Res. 122, 664–669. https://doi.org/10.1161/CIRCRESAHA.117.312465

Liu, T.F., Brown, C.M., El Gazzar, M., McPhail, L., Millet, P., Rao, A., Vachharajani, V.T., Yoza, B.K., McCall, C.E., 2012. Fueling the flame: bioenergy couples metabolism and inflammation. J. Leukoc. Biol. 92, 499–507. https://doi.org/10.1189/JLB.0212078

Liu, Y., Yan, W., Tohme, S., Chen, M., Fu, Y., Tian, D., Lotze, M., Tang, D., Tsung, A., 2015. Hypoxia induced HMGB1 and mitochondrial DNA interactions mediate tumor growth in hepatocellular carcinoma through Toll-like receptor 9. J. Hepatol. 63, 114–121. https://doi.org/10.1016/J.JHEP.2015.02.009

Livak, K.J., Schmittgen, T.D., 2001. Analysis of relative gene expression data using real-time quantitative PCR and the 2(-Delta Delta C(T)) Method. Methods 25, 402–408. https://doi.org/10.1006/METH.2001.1262

Ma, X., Yan, W., Zheng, H., Du, Q., Zhang, L., Ban, Y., Li, N., Wei, F., 2015. Regulation of IL-10 and IL-12 production and function in macrophages and dendritic cells. F1000Research 4, 1–13. https://doi.org/10.12688/F1000RESEARCH.7010.1/DOI

MacMicking, J., Xie, Q.W., Nathan, C., 1997. Nitric oxide and macrophage function. Annu. Rev. Immunol. 15, 323–350. https://doi.org/10.1146/ANNUREV.IMMUNOL.15.1.323

554 Mantovani, A., Sica, A., Sozzani, S., Allavena, P., Vecchi, A., Locati, M., 2004. The
555 chemokine system in diverse forms of macrophage activation and polarization.
556 Trends Immunol. 25, 677–686. https://doi.org/10.1016/J.IT.2004.09.015

557 Martinez, F.O., Sica, A., Mantovani, A., Locati, M., 2008. Macrophage activation and
558 polarization. Front. Biosci. 13, 453–461. https://doi.org/10.2741/2692

559 Mishra, S., Arsh, A.M., Rathore, J.S., 2022. Trained innate immunity and diseases: Bane
560 with the boon. Clin. Immunol. Commun. 2, 118–129.
561 https://doi.org/10.1016/J.CLICOM.2022.08.004

562 Netea, M.G., Domínguez-Andrés, J., Barreiro, L.B., Chavakis, T., Divangahi, M., Fuchs,
563 E., Joosten, L.A.B., van der Meer, J.W.M., Mhlanga, M.M., Mulder, W.J.M.,
564 Riksen, N.P., Schlitzer, A., Schultze, J.L., Stabell Benn, C., Sun, J.C., Xavier, R.J.,
565 Latz, E., 2020. Defining trained immunity and its role in health and disease. Nat.
566 Rev. Immunol. 2020 206 20, 375–388. https://doi.org/10.1038/s41577-020-0285-6

567 Netea, M.G., Quintin, J., Van Der Meer, J.W.M., 2011. Trained immunity: a memory for
568 innate host defense. Cell Host Microbe 9, 355–361.
569 https://doi.org/10.1016/J.CHOM.2011.04.006

570 Ogawa, C., Liu, Y. and Kobayashi, K., 2011. Muramyl dipeptide and its derivatives:
571 peptide adjuvant in immunological disorders and cancer therapy. Curr Bioact
572 Compd. 7(3), 180–197. https://doi.org/10.2174/157340711796817913

573 Park, S.H., Park-Min, K.H., Chen, J., Hu, X., Ivashkiv, L.B., 2011. Tumor necrosis factor
574 induces GSK3 kinase-mediated cross-tolerance to endotoxin in macrophages. Nat.
575 Immunol. 12, 607–615. https://doi.org/10.1038/NI.2043

576 Pashenkov, M. V., Murugina, N.E., Budikhina, A.S., Pinegin, B. V., 2019. Synergistic
577 interactions between NOD receptors and TLRs: Mechanisms and clinical
578 implications. J. Leukoc. Biol. 105, 669–680. https://doi.org/10.1002/JLB.2RU0718-
579 290R

580 Quintin, J., Cheng, S.C., van der Meer, J.W.M., Netea, M.G., 2014. Innate immune
581 memory: towards a better understanding of host defense mechanisms. Curr. Opin.
582 Immunol. 29, 1–7. https://doi.org/10.1016/J.COI.2014.02.006

583 Regdon, Z., Robaszkiewicz, A., Kovács, K., Rygielska, Ż., Hegedűs, C., Bodoor, K.,
584 Szabó, É., Virág, L., 2019. LPS protects macrophages from AIF-independent
585 parthanatos by downregulation of PARP1 expression, induction of SOD2
586 expression, and a metabolic shift to aerobic glycolysis. Free Radic. Biol. Med. 131,
587 184–196. https://doi.org/10.1016/J.FREERADBIOMED.2018.11.034

588 Robinson, N., Ganesan, R., Hegedűs, C., Kovács, K., Kufer, T.A., Virág, L., 2019.
589 Programmed necrotic cell death of macrophages: Focus on pyroptosis, necroptosis,
590 and parthanatos. Redox Biol. 26. https://doi.org/10.1016/J.REDOX.2019.101239

591 Rodríguez-Prados, J.-C., Través, P.G., Cuenca, J., Rico, D., Aragonés, J., Martín-Sanz,
592 P., Cascante, M., Boscá, L., 2010. Substrate fate in activated macrophages: a
593 comparison between innate, classic, and alternative activation. J. Immunol. 185,
594 605–614. https://doi.org/10.4049/JIMMUNOL.0901698

595 Swindall, A.F., Stanley, J.A., Yang, E.S., 2013. PARP-1: Friend or Foe of DNA Damage
596 and Repair in Tumorigenesis? Cancers (Basel). 5, 943–958.
597 https://doi.org/10.3390/CANCERS5030943

598 Taciak, B., Białasek, M., Braniewska, A., Sas, Z., Sawicka, P., Kiraga, Ł., Rygiel, T.,
599 Król, M., 2018. Evaluation of phenotypic and functional stability of RAW 264.7 cell
600 line through serial passages. PLoS One 13.
601 https://doi.org/10.1371/JOURNAL.PONE.0198943

602 Underhill, D.M., 2007. Collaboration between the innate immune receptors dectin-1,
603 TLRs, and Nods. Immunol. Rev. 219, 75–87. https://doi.org/10.1111/J.1600-
604 065X.2007.00548.X

605 Van Ginderachter, J.A., Movahedi, K., Hassanzadeh Ghassabeh, G., Meerschaut, S.,
606 Beschin, A., Raes, G., De Baetselier, P., 2006. Classical and alternative activation
607 of mononuclear phagocytes: picking the best of both worlds for tumor promotion.
608 Immunobiology 211, 487–501. https://doi.org/10.1016/J.IMBIO.2006.06.002

609 Wang, L. xun, Zhang, S. xi, Wu, H. juan, Rong, X. lu, Guo, J., 2019. M2b macrophage
610 polarization and its roles in diseases. J. Leukoc. Biol. 106, 345–358.
611 https://doi.org/10.1002/JLB.3RU1018-378RR

612 Wang, Y., Li, N., Zhang, X., Horng, T., 2021. Mitochondrial metabolism regulates
613 macrophage biology. J. Biol. Chem. 297, 100904.
614 https://doi.org/10.1016/j.jbc.2021.100904

615 Wei, J., Wang, B., Chen, Y., Wang, Q., Ahmed, A.F., Zhang, Y., Kang, W., 2022. The
616 Immunomodulatory Effects of Active Ingredients From Nigella sativa in RAW264.7
617 Cells Through NF-κB/MAPK Signaling Pathways. Front. Nutr. 9.
618 https://doi.org/10.3389/FNUT.2022.899797

619 Xue, Q., Liu, X., Chen, C., Zhang, X., Xie, P., Liu, Y., Zhou, S., Tang, J., 2021. Erlotinib
620 protests against LPS-induced parthanatos through inhibiting macrophage surface
621 TLR4 expression. Cell death Discov. 7. https://doi.org/10.1038/S41420-021-00571-
622 4

623 Yu, X., Wu, B., Lin, Y., Xiong, H.-Y., Xie, C., Liu, C., Li, Z., Tu, Z., 2016.
624 Overexpression of IL-12 reverses the phenotype and function of M2 macrophages
625 to M1 macrophages.

626

627

628 6 **Acknowledgments:** Dr. Ivana Soria and Dr. Fernando Delgado for technical support
629 and Dr. Mariano Perez-Filgueira for critical reading of the manuscript.
630
631 7 **Funding:** This work was funded by the National Institute of Livestock and
632 Agriculture Technologies (INTA). FCM is researcher of INTA; MCM, SSM and
633 AVC are researchers from the National Council for Technical Research (CONICET).
634 **8 Author contributions:** FCM: conceptualization, methodology, formal analysis and
635 visualization, writing original draft; MCM: methodology, data curation, review and

editing; SSM: data curation, validation, review and editing; CPR: methodology, review and editing; AVC: Funding acquisition, Visualization, review and editing.

Declaration of interests

☒The authors declare that they have no known competing financial interests or personal relationships that could have appeared to influence the work reported in this paper.

☐The authors declare the following financial interests/personal relationships which may be considered as potential competing interests: